



Structural study and hydrogen sorption kinetics of ball-milled magnesium hydride

J. Huot^{a,*}, G. Liang^b, S. Boily^a, A. Van Neste^b, R. Schulz^a

^aTechnologies Émergentes de Production et de Stockage, Institut de Recherche d'Hydro-Québec, Varennes, QC, Canada J3X 1S1

^bDépartement de Mines et Métallurgie, Université Laval, Ste-Foy, QC, Canada G1K 7P4

Abstract

It has recently been discovered that energetic ball milling of hydrides can improve their hydrogen sorption properties significantly. In this work, we present a systematic study of structural modifications and hydrogen absorption–desorption kinetics of ball-milled magnesium hydride. Structural investigations showed that after only 2 h of milling, a metastable orthorhombic (γ) magnesium hydride phase is formed. A Rietveld analysis of the X-ray diffraction spectrum of the 20 h milled sample gave a proportion of 74 wt.% MgH_2 , 18 wt.% γ MgH_2 and 8 wt.% MgO . The hydrogen capacity and sorption kinetics were measured before and after milling. We found that the sorption kinetics are much faster for the milled sample compared to the unmilled one. This explains the fact that the hydrogen desorption temperature of the ball-milled sample as measured by pressured differential scanning calorimetry (PDSC), is reduced by 64 K compared to the unmilled sample. There is no significant change of the storage capacity upon milling and the absorption plateau pressure does not change. From the desorption curves, the activation energy was deduced. The milling also increased the specific surface area. This was confirmed by SEM micrographs and BET measurements. Possible mechanisms explaining the improved kinetics are presented. © 1999 Elsevier Science S.A. All rights reserved.

Keywords: Nanocrystalline materials; Magnesium hydride; Ball milling; Hydrogen storage; Kinetics

1. Introduction

Because of its high hydrogen storage capacity (7.6 wt.%), magnesium could be attractive for energy storage material. However, due to the hydride stability and slow sorption kinetics, the actual applications are limited. The sorption kinetics of Mg-based alloys can be improved by the addition of a catalyst such as Pd [1,2], by forming a composite with a low-temperature hydride [3,4] or by using multiphase systems [5]. Other ways to improve sorption properties of magnesium-based hydrogen-storage materials are chemical modifications using organic materials [6] and magnesium–graphite composites [7]. However, these techniques have the drawback of cost increase in the case of palladium and reduced hydrogen capacity for the composites and multiphase systems.

A new and powerful way of improving the hydrogen sorption properties is by energetic ball milling of hydrides [8]. This technique is attractive because it greatly improves absorption–desorption kinetics without the added cost of a catalyst and with minimal loss of storage capacity. In this paper, we present a study on the structural change and

hydrogen sorption kinetics of ball-milled magnesium hydride.

In order to understand the behavior of MgH_2 under milling, the phase diagram of the H–Mg system should be examined. It is well known that, upon hydrogenation, the hydrogen first dissolves in Mg as an interstitial solid solution, forming the hcp α phase [9]. Further hydrogenation produces the tetragonal β - MgH_2 phase. Under high compressive stress, this β phase transforms into a metastable orthorhombic phase (γ) [10,11]. At 293 K and under a pressure of 8 GPa applied for 1 h, a mixture of β and γ phase can be obtained [10]. Upon heating at 623 K, the metastable γ phase totally reverts to the β phase [10]. The β and γ phases are closely related. They have the same packing type and coordination number. In the γ phase, the H octahedron surrounding a Mg atom is deformed and the octahedral chain takes a zigzag form compared to the straight chain in the β phase [10].

2. Experimental details

Pure magnesium hydride (95 wt.% MgH_2 , 5 wt.% Mg) was provided by Th. Goldschmidt AG. The average

*Corresponding author.

particle size was 20 μm as reported by the manufacturer. The milling was carried out with a Spex 8000 model shaker mill and a vial and balls of stainless steel with a ball to powder weight ratio of 10:1. Milling times for up to 20 h were used. At regular intervals, a small amount of powder was taken for analysis. The X-ray powder diffraction was performed on a Siemens D500 apparatus with $\text{CuK}\alpha$ radiation. For X-ray diffraction under hydrogen pressure, we used a Philips X'pert system ($\text{CuK}\alpha$ radiation) with an Anton Paar XRK9000 pressurized sample holder. Before measurement, the system was flushed with hydrogen for 15 min. A hydrogen pressure of 2 bar was then established. The X-ray diffraction patterns were analyzed using the Rietveld method and RIETAN software [12]. Lattice parameters, phase abundance, crystallite size and strain were extracted from the Rietveld refinement output. Oxygen content was measured with a LECO TC-136 apparatus. Iron content was measured with an optical spectrometer from Jarrel-Ash, model ICAP 9000. The thermal behavior was studied by pressurized differential scanning calorimeter (PDSC) using a TA 2190 calorimeter with a chromel–alumel thermocouple at a heating rate of 10 K min^{-1} under 2 bar of hydrogen. Field emission scanning electron micrographs were taken on a Hitachi model S4700. The specific surface area was measured with an Autosorb 1 apparatus from Quantachrome using the BET method with nitrogen gas.

The hydrogen storage properties of the mechanically milled powders were evaluated by using an automatic Sieverts apparatus. The magnesium hydride powders after 20 h of milling were put into the reactor, and pumped for 20 min, then heated to 623 K to do the desorption. The first desorption was very rapid at this temperature. There

was no change in absorption and desorption kinetics on cycling. After 10 absorption and desorption cycles, the kinetic curves at various temperatures were then measured.

3. Results and discussion

3.1. Formation of γ phase

The powder diffraction patterns of ball-milled MgH_2 as a function of milling time are shown in Fig. 1. After 2 h of milling there is a formation of $\gamma\text{-MgH}_2$ and the appearance of MgO . All peaks are broad, indicating a small crystallite size. Further milling did not change the abundance of the phases significantly. This formation of a metastable phase synthesized at room temperature by ball milling has also been seen in many other systems such as in the case of the iron anhydrous ammonia system [13]. The high energy impact of the balls increases the free energy of the system by creating deformations and structural defects in the material. The high free energy allows us to overcome the activation energy barrier to form the metastable phase [13].

In Fig. 2, we present the Rietveld refinement of a powder diffraction pattern taken under 2 bar of hydrogen at 323 K. The small residue indicates an excellent fit. Quantitatively, the goodness of the fit is expressed by R_{wp} , the weighted difference between the calculated and the measured intensities and by R_e which is an estimation of the minimum value of R_{wp} . In the present case, $R_{\text{wp}}=7.9\%$ and $R_e=4.9\%$. The goodness of the fit for a particular phase is indicated by the R_{Bragg} (R_B) value. For the fit of Fig. 2, the R_B of $\beta\text{-MgH}_2$, $\gamma\text{-MgH}_2$ and MgO were,

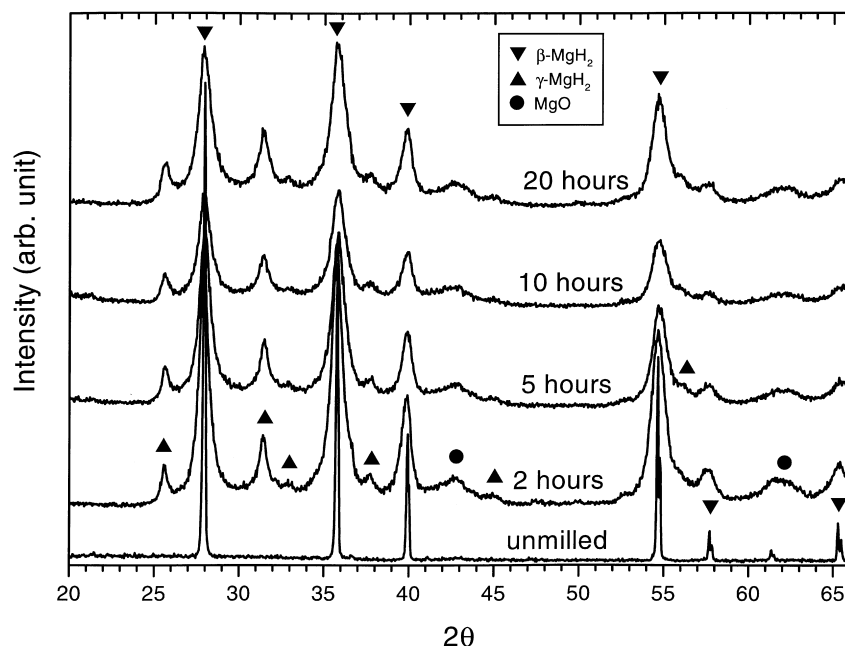


Fig. 1. X-ray powder diffraction of nanocrystalline MgH_2 as a function of the milling time. ▼, $\beta\text{-MgH}_2$; ▲, $\gamma\text{-MgH}_2$; ●, MgO .

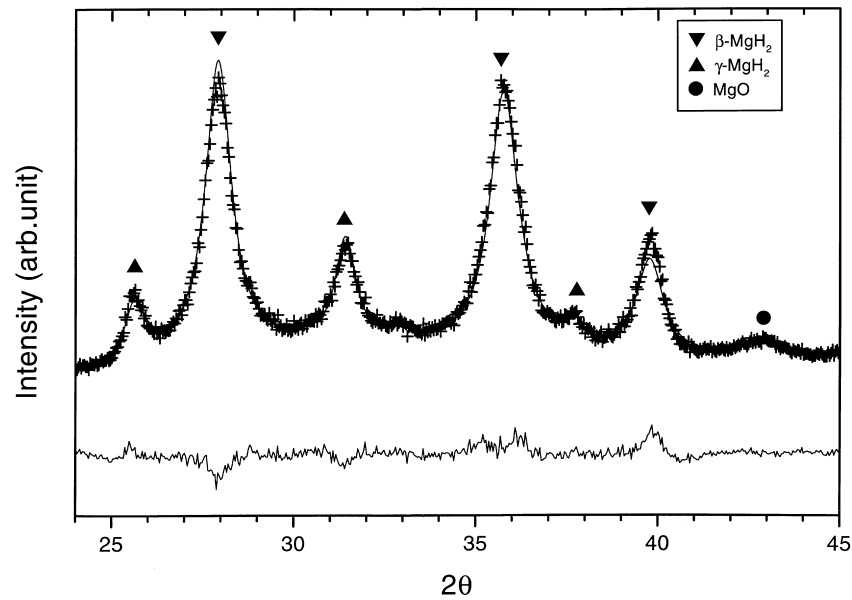


Fig. 2. Rietveld refinement of the X-ray powder diffraction of ball-milled MgH_2 taken under 2 bar of hydrogen. Crosses are experimental values, the solid line is the calculated intensity and the bottom line is the residue. ∇ , $\beta\text{-MgH}_2$; \blacktriangle , $\gamma\text{-MgH}_2$; \bullet , MgO .

respectively, 2.8%, 1.7% and 1.6%. These values suggested a very good fit for each individual phase.

The abundance, crystallite size and strain of each phase are reported in Table 1. As seen in the diffraction patterns of Fig. 1, the $\gamma\text{-MgH}_2$ phase abundance of 18 wt.% did not increase after 2 h of milling time. Therefore, during milling there should be two competing processes, one promoting the formation of the γ phase (the mechanically driven $\beta \rightarrow \gamma$ transformation), the other favoring the presence of the β phase (thermally driven $\gamma \rightarrow \beta$ transformation). As shown in Table 1, the residual strain value of the γ and β phases is relatively high. The γ and β phases being closely related, the γ phase can be seen as a small distortion of the β phase. Another possible explanation of the constant abundance of the γ and β phases might be that during milling, the increase of strain in the γ phase beyond a certain level induces a strain relaxation process which gives rise to a $\gamma \rightarrow \beta$ transformation. More work is needed to elucidate this point.

The appearance of MgO was due to the presence of oxygen in the starting powder and the high reactivity of milled MgH_2 . The proportion of oxygen before and after milling 20 h was measured to be 0.6 wt.% and 1.4 wt.%,

Table 1

Phase abundance, strain and crystallite size deduced from Rietveld refinement of the X-ray diffraction pattern of the MgH_2 milled for 20 h^a

Phase	Abundance (wt.%)	Strain (%)	Crystallite size (nm)
$\gamma\text{-MgH}_2$	18(2)	1.18(4)	17.1(7)
$\beta\text{-MgH}_2$	74(3)	1.12(2)	11.9(1)
MgO	8(1)	–	6.7(3)

^a Values in parentheses are three standard deviations.

respectively. In the unmilled powder, the oxygen is present in the form of a thin layer of MgO on the surface of the particles and is hard to detect by X-ray diffraction. This fact was proved for other systems [14,15]. By milling, the crystallite size of MgO is reduced. The increase of oxygen during milling is due to the high reactivity of magnesium. Because the reduction potential of Mg is very low, the small fraction (5 wt.%) of pure magnesium present in the starting powder can easily reduce oxides within the crucible and form MgO .

3.2. Hydrogen sorption properties

The desorption curves of the unmilled commercial and ball-milled MgH_2 under vacuum (0.01 MPa hydrogen pressure) are shown in Fig. 3. The desorption of unmilled MgH_2 is very slow. There is no obvious desorption at 573 K within 2000 s. Even at 623 K, it takes more than 3000 s to desorb completely. In comparison, the desorption of the ball-milled magnesium hydride is much more rapid. It can fully desorb at 623 K in about 700 s. Although the desorption at 573 K is slower, it can still desorb about 2.2 wt.% of hydrogen within 2000 s.

Both the unmilled and ball-milled MgH_2 give a similar sigmoidal desorption curve. This means that a nucleation and growth process takes place during desorption. By fitting the desorption curves with the Johnson-Mehl-Avrami (JMA) equation [16]: where

$$\alpha = 1 - \exp\{- (Kt)^\eta\}$$

η is the reaction exponent, α is the desorption fraction at time t , $K = K_0 \exp(-Q/RT)$, Q is the activation energy, R

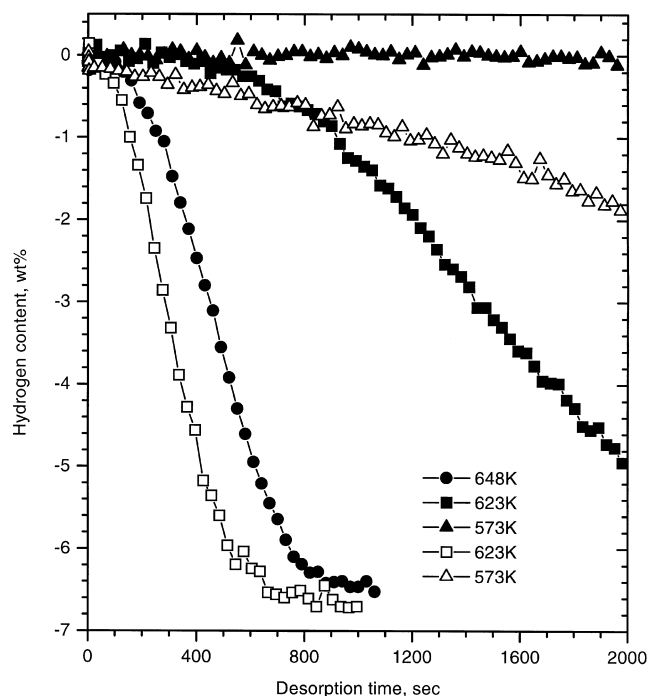


Fig. 3. Hydrogen desorption curves of unmilled MgH_2 (filled marks) and ball-milled (hollow marks) MgH_2 under a hydrogen pressure of 0.015 MPa.

is the gas constant and T is the temperature. We found for the milled and unmilled powder a value of $\eta=3$. This value can be interpreted as an instantaneous nucleation followed by an interface-controlled three-dimensional growth process.

Using the JMA equation, the rate constant K can also be determined by fitting the desorption curve. From the Arrhenius plot of K values with temperature, the activation energies of desorption for the ball-milled and unmilled MgH_2 are found to be 120 and 156 kJ/mol K, respectively.

As shown in Fig. 4 the hydrogen absorption kinetics is also greatly improved by intensive milling. The desorbed unmilled commercial material can only be rehydrogenated slowly at elevated temperatures. There is no obvious absorption below 423 K. Even at 573 K, it takes 3000 s to reach half of the maximum storage capacity under a hydrogen pressure of 1.0 MPa. The ball-milled material on the other hand can fully absorb hydrogen at 573 K in 750 s. The absorption is also fast at lower temperatures. This excellent kinetic behavior does not deteriorate by cycling at high temperature (623 K). The absorption is mainly controlled by diffusion because the diffusion of hydrogen in the β phase is much slower than in the α phase [17].

As is well known, the hydrogen absorption kinetics of magnesium can be improved significantly by alloying [18,19]. It was reported that additions of small amount of In, Al and Ga to magnesium reduced the activation energy of hydrogenation [20]. The catalytic effect of iron on the Mg–H reaction was also observed [14]. In the present

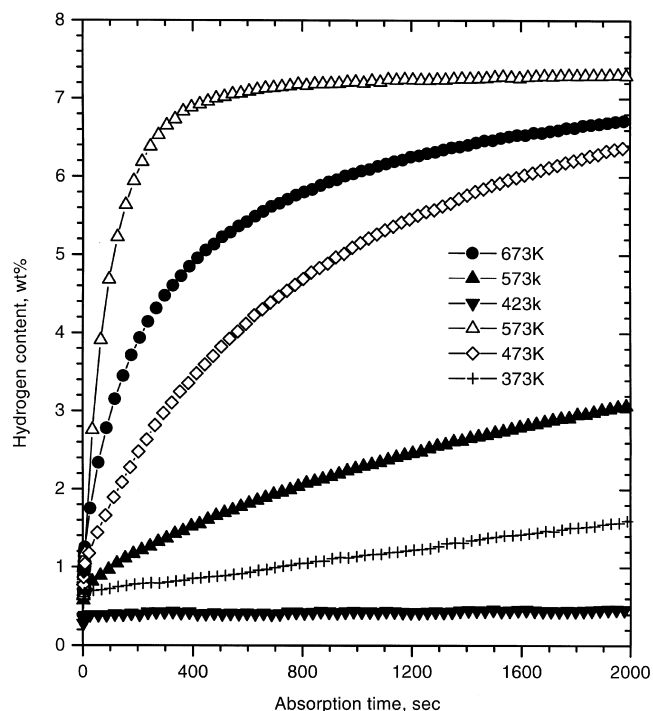


Fig. 4. Hydrogen absorption curves of the unmilled (filled marks) and ball-milled (hollow marks) MgH_2 under a hydrogen pressure of 1.0 MPa.

case, the iron impurity content in the milled sample was measured by chemical analyses to be about 0.13 wt.%. We consider that such a small amount of Fe could not contribute much to the improvement of kinetics.

The orthorhombic metastable (γ) magnesium hydride phase disappeared upon hydrogen cycling. The X-ray spectrum shows that only β - MgH_2 remains after partial rehydrogenation at 473 K with some residual Mg peaks. The kinetics does not change with the disappearance of γ - MgH_2 . After desorption, strong magnesium peaks and small MgO peaks are present.

The pressure–concentration–temperature (PCT) curves for both milled and unmilled MgH_2 have also been measured. The absorption plateau pressure remains the same before and after milling, as shown in Fig. 5. The maximum hydrogen content decreases slightly after ball milling due to the formation of MgO. The desorption pressure of the unmilled MgH_2 is lower than that of the milled one or of other reported magnesium alloys [9] because the desorption kinetics is slow and the real equilibrium is not reached. These measurements indicate that the thermodynamic properties of magnesium hydride are not altered by mechanical milling.

3.3. Particle size and specific surface area

The specific surface area before and after milling was $1.2 \text{ m}^2 \text{ g}^{-1}$ and $9.9 \text{ m}^2 \text{ g}^{-1}$, respectively, as measured using the BET method. This important increase of specific surface area was confirmed by the SEM micrographs

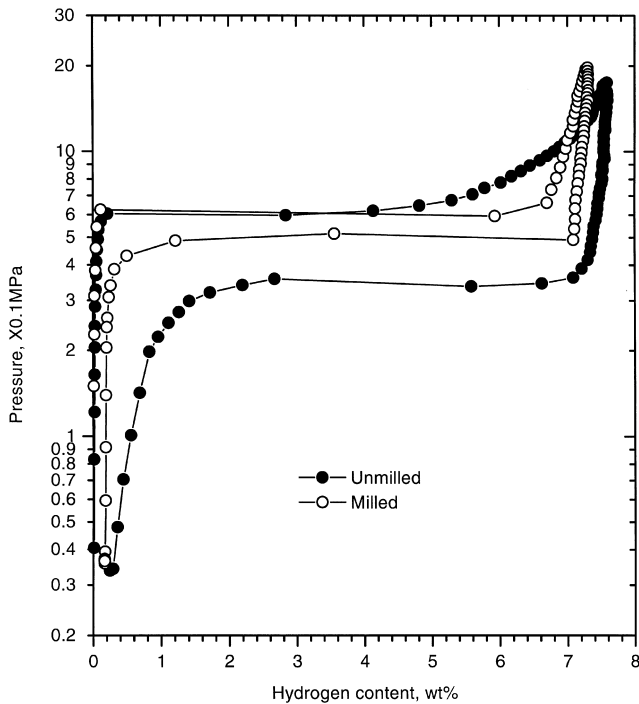


Fig. 5. Pressure–concentration–temperature curves of the un-milled and ball-milled MgH_2 at 623 K.

presented in Fig. 6. Before milling, each particle was a solid block of MgH_2 with a smooth surface. After milling the particles were smaller. In the ball-milled powder, the bigger particles were agglomerations of much smaller particles and their surfaces were full of asperities.

3.4. Calorimetric measurements

In Fig. 7, we present the PDSC traces of un-milled and 20 h milled samples. The desorption peak is reduced by 64 K after milling and becomes a double peak. However, from the MgH_2 heat of formation [9], a plateau pressure of 2 bar (pressure at which the PDSC experiment was

conducted) corresponds to a temperature of 578 K which is still below the onset of desorption peak after milling. Therefore, the shift of peak temperature reflects an increase in the hydrogen sorption kinetics and a reduction of activation energy rather than a change in the thermodynamic properties. This conclusion is supported by equilibrium pressure–composition measurements reported in Section 3.2. The splitting of the desorption peak is under investigation.

4. Conclusion

Energetic ball milling of magnesium hydride at room temperature has the following effects:

1. Formation of nanocrystalline metastable $\gamma\text{-MgH}_2$ phase with a proportion of 18 wt.%. The $\beta\text{-MgH}_2$ phase also becomes nanocrystalline with a smaller crystallite size than the $\gamma\text{-MgH}_2$ phase.
2. After milling, the particles were agglomerations of smaller particles. The surfaces of the milled particles were very rough compared to the un-milled ones. This was accompanied by a 10-fold increase in the specific surface area.
3. The hydrogen desorption temperature, as measured using a differential scanning calorimeter, was reduced by 64 K. This indicates faster hydrogen desorption kinetics and a reduced activation energy.
4. The hydrogen sorption kinetics of magnesium hydride can be improved by ball milling. The ball-milled magnesium hydride could fully absorb at 573 K and desorb at 623 K within a few minutes, which is 5 times faster than that of un-milled MgH_2 . The improved kinetics is explained by the defects introduced during ball milling, the small particle size and by the increased specific surface area which increases the nucleation site density and reduces the diffusion lengths.

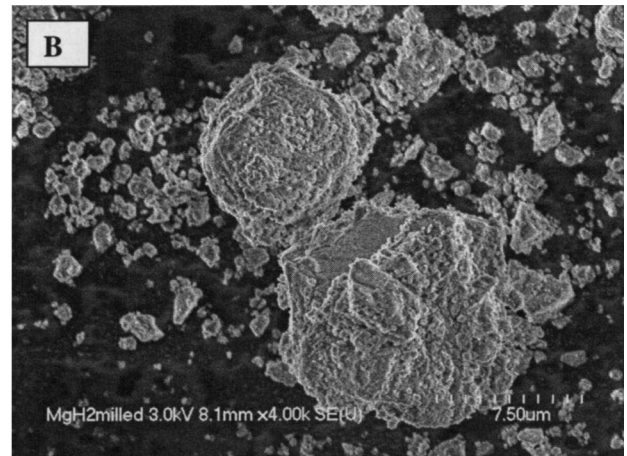
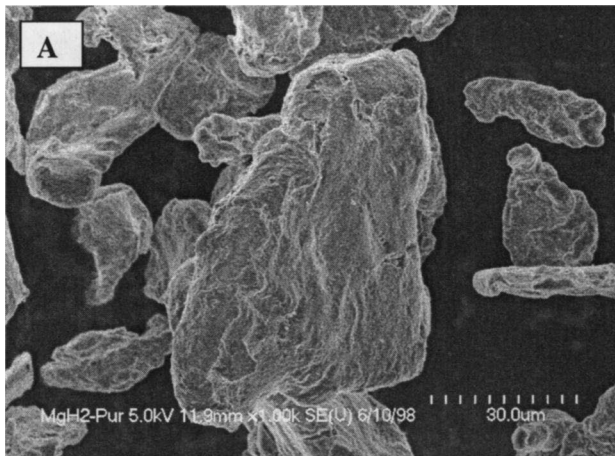


Fig. 6. SEM micrographs of MgH_2 before (A) and after milling for 20 h (B).

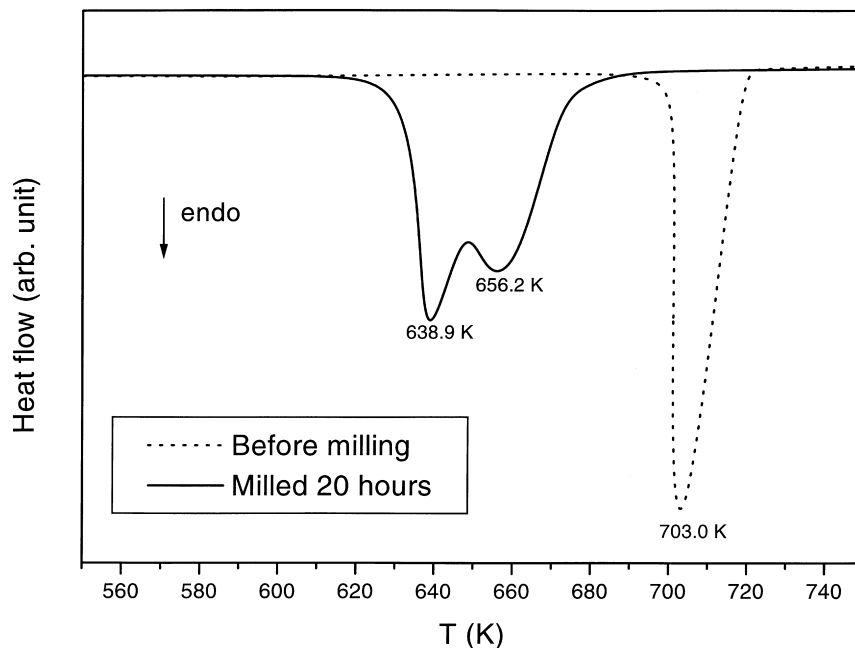


Fig. 7. PDSC trace of MgH_2 before and after 20 h of milling.

5. The activation energy for desorption was measured to be 120 and 156 kJ mol^{-1} for the milled and unmilled powders. Intensive milling does not alter the thermodynamic properties of magnesium hydride.

References

- [1] L. Zaluski, A. Zaluska, P. Tessier, J.O. Strom-Olsen, R. Schulz, *J. Alloys Comp.* 217 (1995) 295.
- [2] L. Zaluski, A. Zaluska, J.O. Strom-Olsen, *J. Alloys Comp.* 253–254 (1997) 70.
- [3] B. Tanguy, J.-L. Soubeyroux, M. Pezat, J. Portier, P. Hagenmuller, *Mat. Res. Bull.* 11 (1976) 1441.
- [4] G. Liang, S. Boily, J. Huot, A. Van Neste, R. Schulz, *J. Alloys Comp.* 268 (1998) 302.
- [5] G. Liang, S. Boily, J. Huot, A. Van Neste, R. Schulz, *J. Alloys Comp.* 267 (1998) 302.
- [6] H. Imamura, *J. Less-Common Met.* 172–174 (1991) 1064.
- [7] H. Imamura, N. Sakasai, T. Fujinaga, *J. Alloys Comp.* 253–254 (1997) 34.
- [8] A. Zaluska, L. Zaluski, J.O. Strom-Olsen, R. Schulz, US Patent Application No. US08-645 352.
- [9] J.F. Stampfer, C.E. Holley, J.F. Suttle, *J. Am. Chem. Soc.* 82 (1960) 3504.
- [10] J.-P. Bastide, B. Bonnetot, J.-M. Letoffe, P. Claudy, *Mat. Res. Bull.* 15 (1980) 1215.
- [11] A.A. Nayeb-Hashemi, J.B. Clark (Eds.), *Phase Diagrams of Binary Magnesium Alloys*, ASM International, Metals Park, OH, 1988.
- [12] F. Izumi, Rietveld analysis programs RIETAN and PREMOS and special applications, in: R.A. Young (Ed.), *The Rietveld Method*, Oxford University Press, Oxford, 1993.
- [13] Y. Chen, J.S. Williams, G.M. Wang, *J. Appl. Phys.* 78 (1996) 3956.
- [14] E. Ivanov, I. Konstanchuk, A. Stepanov, V. Boldyrev, *J. Less-Common Met.* 131 (1987) 25.
- [15] A. Calka, J.I. Nikolov, *J. Appl. Phys.* 75 (1994) 4953.
- [16] P.S. Rudman, *J. Less-Common Met.* 89 (1983) 93.
- [17] J. Topler, H. Buchner, H. Saufferer, H. Knorr, W. Prandl, *J. Less-Common Met.* 88 (1982) 397.
- [18] D.L. Douglass, *Metallurgical Transactions A* 6A (1975) 2179.
- [19] N. Gerard, S. Ono, *Hydride formation and decomposition kinetics*, in: L. Schlapbach (Ed.), *Hydrogen in Intermetallic Compounds II, Topics in Applied Physics*, Vol. 67, Springer-Verlag, Berlin, 1992, Chap. 4.
- [20] M.H. Mintz, Z. Gavra, Z. Hadari, *J. Inorg. Nucl. Chem.* 40 (1978) 765.